Giant Dipole Resonance in Highly Excited Nuclei: Does the Width Saturate?

M. P. Kelly, K. A. Snover, and J. P. S. van Schagen
Nuclear Physics Laboratory, University of Washington, Seattle, Washington 98195

M. Kicińska-Habior and Z. Trznadel
Institute of Experimental Physics, Warsaw University, 00-681 Warsaw, Poland
(Received 2 November 1998)

We examine the behavior of the width of the giant dipole resonance (GDR) at high excitation energies and show, based on new detailed measurements together with a reanalysis of previous experimental results, that the GDR width in Sn and nearby mass compound nuclei continues to increase up to final-state temperatures $T \sim 3.2$ MeV. These temperatures correspond to the highest energies at which the GDR width can be extracted reliably from existing data. [S0031-9007(99)08845-6]

PACS numbers: 24.30.Cz, 24.60.Dr, 25.70.Gh, 27.60.+j

One of the outstanding questions in nuclear physics is the behavior of the width of the giant dipole resonance (GDR) built on excited states at high excitation energy: does it saturate? In fusion-evaporation reactions at low energies corresponding to nuclear temperatures $T \leq 2$ MeV, the width is observed to increase rapidly with bombarding energy due to increasing spin-induced deformation, and increasing thermal shape fluctuations [1,2]. In this regime the global systematics of the GDR width are described reasonably well by shape fluctuation calculations in which the quadrupole deformation of the nucleus is assumed to couple adiabatically to the GDR vibration (see, e.g., Ref. [3]). Beyond the bombarding energy at which the angular momentum saturates (the maximum angular momentum the nucleus can sustain without fissioning) it has been argued [4] that the GDR width should grow much more slowly. Previous experiments [2,4–6] (see also Ref. [7]) have been interpreted in terms of a saturating width and, at higher bombarding energies, a saturating GDR γ-ray multiplicity (number of high-energy γ rays per compound nucleus). However, at high bombarding energy it is difficult to know the initial excitation energy of the decaying nuclei, which greatly complicates the interpretation of these experiments.

In this Letter, we present results of angular distribution measurements of preequilibrium protons and α particles, evaporative protons and α particles, and evaporation residues [8] and multiplicity-gated high-energy photons produced in ^{18}O + ^{100}Mo collisions at $E(^{18}\mathrm{O}) =$ 122 to 214 MeV [9], spanning the interesting energy range where the GDR width is claimed to saturate. We find substantial preequilibrium emission over most of this energy range, in contrast to assumption in previous GDR decay experiments. Using the forward/backward γ-ray anisotropy to constrain the bremsstrahlung yield underlying the GDR, we are able to extract with confidence the GDR parameters and the final-state temperatures corresponding to GDR emission. We find that the GDR width is still increasing over this energy range, corresponding to temperatures T up to 2.4 MeV. We also reinterpret the results of previous experiments at similar and somewhat higher energies and show that they are consistent with an increasing width up to $T \sim 3.2$ MeV once one accounts for larger preequilibrium losses than previously assumed.

^{118}Sn and nearby mass compound nuclei were produced with a pulsed ^{18}O beam from the University of Washington Nuclear Physics Laboratory tandem-linac accelerator and 0.8–3.1 mg/cm^2 isotopically enriched ^{100}Mo targets. High-energy γ rays were detected in three large NaI spectrometers, and low-energy γ-ray multiplicities were measured using 22 small NaI crystals covering approximately 20% of 4π. The center-of-mass γ-ray angular distributions were assumed to have the form $\sigma(\theta_{\mathrm{cm}}) = A_0[1 + a_1 P_1(\cos(\theta_{\mathrm{cm}})) + a_2 P_2(\cos(\theta_{\mathrm{cm}}))]$, based on the dominance of electric dipole radiation. The $a_1(E_\gamma)$ coefficients, which must be zero for statistical emission, are nonzero at high E_γ due to bremsstrahlung emission, indicating significant bremsstrahlung at bombarding energies as low as 122 MeV (6.8 MeV/nucleon). The $a_2(E_\gamma)$ coefficients are small and not well determined.

We use separate ^{18}O + ^{100}Mo measurements [8] to determine preequilibrium energy and mass losses. For processes leading to fusion, the average excitation energy lost relative to complete fusion is 21% for 197 MeV bombarding energy (11 MeV/nucleon). A second point corresponding to 15% loss at 166 MeV was estimated by scaling the measured losses at 197 MeV by the (unpublished) ratios of measured singles preequilibrium cross sections at 166 and 197 MeV for protons and for α's (neutron losses were assumed to scale with proton losses). A straight line fit to the corresponding reduced excitation energies (see Fig. 3) shows the average initial excitation energy of the compound system. The excitation energy loss is given by $\Delta E_x(\mathrm{MeV}) = 8.7[(E_{\mathrm{proj}} - V_c)/A_{\mathrm{proj}}] - 33$ where the Coulomb barrier $V_{\mathrm{c}} = 52.5$ MeV for ^{18}O + ^{100}Mo. As noted before [8], these excitation energy losses are much larger than the corresponding amount of lost linear momentum transfer (e.g., 8% at 11 MeV/nucleon). The losses are also much larger than assumed previously, due partly to underestimates of the binding energy contribution to the loss.

The average excitation energy, mass, and Z of the populated compound nuclei, corrected for preequilibrium loss, were used in CASCADE statistical model calculations with the Reisdorf [10,11] level density description and a single Lorentzian GDR strength function. Measured residue cross sections [8] were used for the initial fusion cross sections. The GDR and bremsstrahlung parameters were determined by simultaneous fits of the statistical contribution plus a bremsstrahlung component to the measured 90° cross section and $a_1(E_\gamma)$ coefficients.

A parametrization of the bremsstrahlung cross section as a simple exponential, with isotropic emission in a reference frame moving with $0.5v_{\mathrm{beam}}$ as has been established for nucleon-nucleon bremsstrahlung at higher bombarding energies [12], is adequate to describe the measured cross section, but fails to account for $a_1(E_\gamma)$ at all bombarding energies, as shown for 197 MeV bombarding energy in Fig. 1. Several other bremsstrahlung parametrizations give good fit results, such as a "curved" bremsstrahlung cross section given by [13] $\sigma_{\mathrm{brems}} = k(1 - x^2)^\alpha/x$ in the source frame, with $v_{\mathrm{source}} = 0.5v_{\mathrm{beam}}$. Here k, α, and E_{lim} are fit parameters and $x = E_\gamma/E_{\mathrm{lim}}$. Similar quality fits are obtained with $\sigma_{\mathrm{brems}} = k/(A + e^{E_\gamma/E_0})$ and $v_{\mathrm{source}} = 0.5v_{\mathrm{beam}}$, or $\sigma_{\mathrm{brems}} = k \cdot e^{(-E_\gamma/E_0)}$ with a source velocity varying from $\sim 0.3v_{\mathrm{beam}}$ at $E_\gamma = 20$ MeV to $\sim 0.6v_{\mathrm{beam}}$ at $E_\gamma = 30$ MeV. The fitted GDR parameters don't depend strongly on the bremsstrahlung parametrization; however, it is important to include bremsstrahlung in the analysis. Fit results using the curved parametrization are shown in Fig. 1, right panel, and in Fig. 2.

High-energy γ-ray spectra and $a_1(E_\gamma)$ coefficients obtained with a fold ≥4 condition are shown in Figs. 1 and 2 for all five bombarding energies, together with CASCADE plus bremsstrahlung fits to the region $E_\gamma = 11-38$ MeV. Divided plots in the bottom row provide an approximate way of removing the effect of the nuclear level density so that the fitted absorption cross section may be compared to the data on a linear scale.

We use a fold ≥4 multiplicity cut to ensure clean spectra by eliminating noncompound nucleus background. Such background is evident in the fold ≥0 (ungated) data for $E_\gamma < 11$ MeV (not shown), where $a_1(E_\gamma)$ is positive due to some nonequilibrium process such as γ decay of projectilelike fragments (in this low energy region, bremsstrahlung is negligible). There is also some background near $E_\gamma = 15$ MeV from decay of ^{12}C fragments. The background is strongly suppressed by the multiplicity cut, as evidenced by the reduction of the $a_1(E_\gamma)$. For the fold-gated data, shown in Fig. 2, $a_1(E_\gamma)$ is nearly zero on the low side of the GDR, as expected

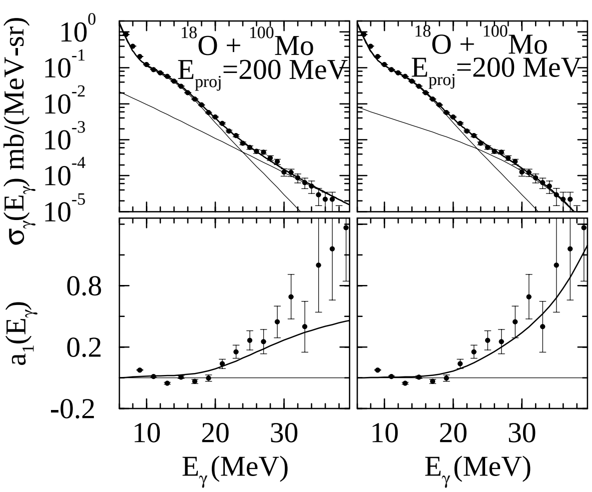

FIG. 1. Simultaneous fit of CASCADE plus bremsstrahlung to the 90° cross section and $a_1(E_\gamma)$. Left column: Exponential bremsstrahlung shape. Right column: Curved bremsstrahlung shape (see text).

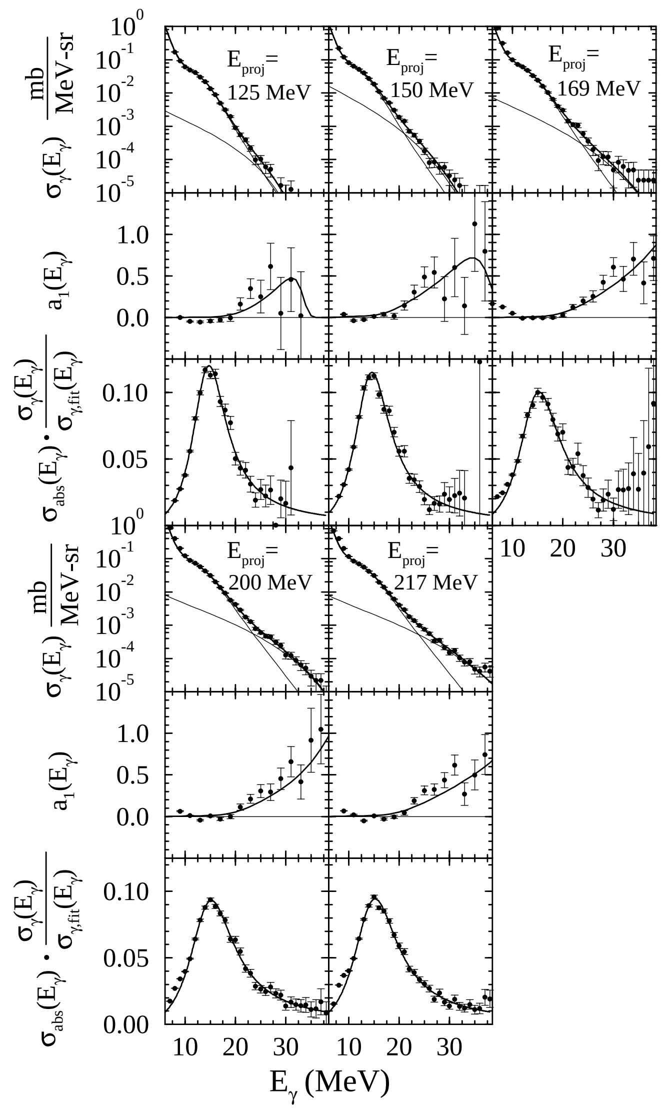

FIG. 2. Measured data and CASCADE plus bremsstrahlung fits. First and fourth rows: 90° γ-ray production cross sections. Second and fifth rows: $a_1(E_\gamma)$ coefficients. Third and sixth rows: Divided plots.

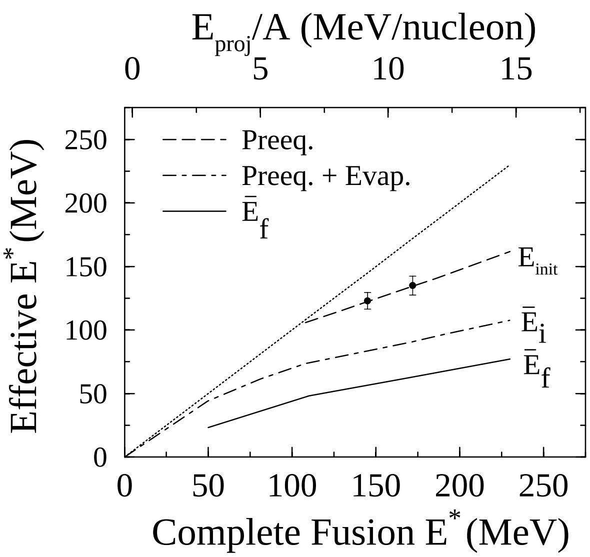

FIG. 3. ^{18}O + ^{100}Mo energetics. Dotted line: Complete fusion excitation energy. Dashed line: Initial compound nucleus energy $E_{\rm init}$ following preequilibrium emission. Dot-dashed line: Average energy $\overline{E}_i$ preceding GDR decay. Solid line: Average thermal energy $\overline{E}_f$ following GDR decay.

for nearly pure statistical decay in the presence of a small bremsstrahlung yield. A further check on our insensitivity to nonstatistical background comes from a comparison of GDR parameters from fits to the fold ≥4 and to the fold ≥0 data, which are similar.

The energetics of our reactions are shown in Fig. 3. The dotted line represents the complete fusion energy, which ranges from 108 to 186 MeV in our measurements. As discussed above, $E_{\rm init}$ represents the initial compound nucleus excitation energy following preequilibrium emission. $\overline{E}_i$ includes the additional energy lost on average by particle evaporation prior to GDR decay, calculated using CASCADE. $\overline{E}_f$ represents the average thermal energy for GDR decay, obtained from $\overline{E}_i$ by subtracting the 15 MeV γ-ray decay energy and the rotational energy. Note that $\overline{E}_f$ is small and increases more slowly with bombarding energy than does $E_{\rm init}$. Note also, if the $\overline{E}_f$ curve flattens out at higher energies, then the GDR width and γ-ray yield will saturate with bombarding energy. In order to interpret properly the GDR parameters, we calculate the average temperature associated with GDR decay, given by $T = [d\ln(\rho)/dE]^{-1}$ evaluated at $E = \overline{E}_f$. This is the temperature relevant to thermal fluctuation calculations of dipole absorption by a heated nucleus [1].

Fitted parameters are shown in Table I together with the deduced temperatures. The GDR strengths all lie in the range 1.1 to 1.3 times the classical dipole sum rule, in good agreement with the value of 1.26 deduced from ground-state photoabsorption on ^{118}Sn [14]. Reasonable agreement (within ±5%) is also found for the resonance energies compared to the ground-state GDR value of 15.4 MeV. Neither the strength nor centroid energy varies significantly with temperature. These results represent the best test to date of the expectation that the strength and resonance energy of the GDR built on excited states should be the same as for the GDR built on the ground state, since all significant parameters relevant to the present determination—initial excitation energy, fusion cross section, and level density parameter [15]—have been measured.

The GDR widths for $T = 2.1$ to 2.4 MeV from the present study are shown in Fig. 4 together with results from previous fusion-evaporation experiments [16–19] at lower excitation energies where preequilibrium effects are small (see also [20]). Where necessary we have recomputed the temperatures corresponding to the previous measurements. As can be seen, the GDR width is still increasing in this range. Also shown in Fig. 4, top panel, is the average angular momentum at the time of GDR decay for ^{18}O + ^{100}Mo reactions calculated using CASCADE (a similar curve is found for the other fusion-evaporation reactions).

We can use our ΔE_x relation for preequilibrium energy loss to correct higher energy GDR data [4–6], based on a demonstrated scaling of preequilibrium emission with $(E_{\rm proj} - V_c)/A_{\rm proj}$ [21] which is insensitive to the projectile/target combination [22]. Our results suggest larger losses than previously assumed, which lower the computed temperatures and raise the estimated GDR widths; the latter occurs because the spectra must be refit with

TABLE I. GDR and bremsstrahlung fit parameters. The strength S is from fold ≥0 data while all other parameters are from fold ≥4 data. $E_{\rm init}$, E_D, Γ, $E_{\rm lim}$, and T are in units of MeV. Errors on GDR parameters include uncertainty in level density, energy calibration, and absolute normalization.

$E_{\rm proj}$	122 MeV	147 MeV	166 Mev	197 MeV	214 MeV
$E_{\rm init}$	107	116	123	134	141
S	1.2 ± 0.2	1.1 ± 0.2	1.3 ± 0.2	1.2 ± 0.2	1.2 ± 0.2
E_D	14.8 ± 0.5	14.6 ± 0.5	15.2 ± 0.5	15.2 ± 0.5	15.2 ± 0.5
Γ	8.3 ± 0.4	8.7 ± 0.4	10.0 ± 0.5	10.7 ± 0.4	10.6 ± 0.4
k	.004 ± .007	.02 ± .005	.008 ± .003	.009 ± .003	.007 ± .002
α	3.5 ± 3.6	7.4 ± 3.3	6.8 ± 4.2	3.9 ± 2.0	6.2 ± 4.5
$E_{\rm lim}$	35 ± 8	43 ± 6	50 ± 10	45 ± 6	56 ± 14
χ^2/ν	1.4	2.0	1.3	1.4	2.2
T	2.14	2.21	2.26	2.36	2.42

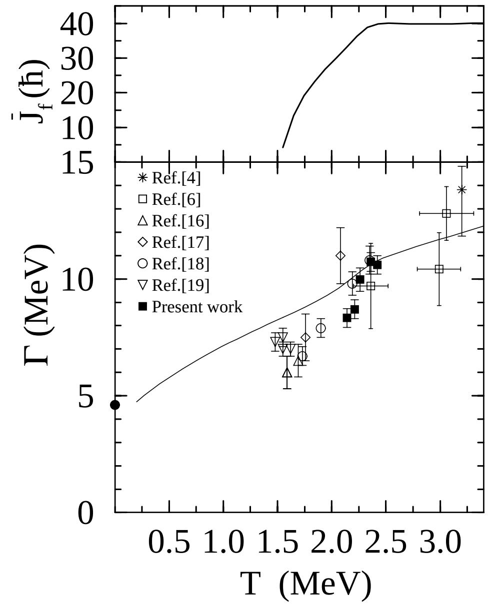

FIG. 4. Decay of Sn and nearby mass compound nuclei. Top panel: Average angular momentum for GDR decay in $^{18}O + ^{100}Mo$. Bottom panel: Points—measured GDR widths; solid line—thermal fluctuation calculation [3,28]. Horizontal axis: Final-state temperature.

CASCADE at a lower excitation energy. For the data of Ref. [4], with a corrected $E_{\rm init} = 206$ MeV ($\overline{E}_i = 137$ MeV), the width correction is small, and the result is plotted at a computed temperature of 3.2 MeV. For the deep-inelastic results of Ref. [6] we use a Fermi jet model calculation [23] to estimate ΔE_x losses due to preequilibrium emission of 10%, 11%, and 27% for the three TKEL bins. The 27% loss for the highest TKEL bin, corresponding to $E_{\rm init} = 244$ MeV ($\overline{E}_i = 157$ MeV) for the Xe-like fragment, is in good agreement with the value 24% obtained from our relation for ΔE_x for heavy-ion fusion, as expected for near-central deep-inelastic collisions, and is much larger than previously assumed. For the two lowest TKEL bins, the energy losses and hence the width corrections are small. These corrected data are also shown in Fig. 4. The inclusion of these higher energy points provides additional evidence for an increasing GDR width up to $T \sim 3.2$ MeV [24]. We note that data at even higher bombarding energy [25–27] do not appear to bear on the issue of width saturation due to the apparent saturation of the GDR γ-ray multiplicity.

The adiabatic thermal fluctuation calculations of Kusnezov and Alhassid [3,28] evaluated at the average angular momentum associated with GDR decay are shown in Fig. 4. Theoretically the absence of width saturation in this energy region results because thermal shape fluctuations are still rising with increasing T and are appreciable compared to the spin-driven broadening.

In conclusion, the results of our study together with a reanalysis of other relevant data nuclei show evidence for a GDR width which continues to increase up to $T \sim 3.2$ MeV in the Sn mass region. Calculations based on the thermal shape fluctuations of a heated rotating liquid drop are in reasonable agreement with the data except at lower energies (temperatures) where the data lie somewhat lower. In order to understand the GDR properties at higher energies and temperatures than those presented here, it is essential to have a reliable measure of the excitation energy of the decaying nuclei.

We acknowledge helpful comments from R. Vandenbosch and the early participation of D. Ye.

[1] K. A. Snover, Annu. Rev. Nucl. Part. Sci. **36**, 545 (1986).
[2] J. J. Gaardhøje, Annu. Rev. Nucl. Part. Sci. **42**, 483 (1992).
[3] D. Kusnezov, Y Alhassid, and K. A. Snover, Phys. Rev. Lett. **81**, 542 (1998).
[4] A. Bracco *et al.*, Phys. Rev. Lett. **62**, 2080 (1989).
[5] H. J. Hofmann *et al.*, Nucl. Phys. **A571**, 301 (1994).
[6] G. Enders *et al.*, Phys. Rev. Lett. **69**, 249 (1992).
[7] D. Pierroutsakou *et al.*, Nucl. Phys. **A600**, 131 (1996).
[8] M. P. Kelly *et al.*, Phys. Rev. C **56**, 3201 (1997).
[9] All projectile energies are quoted at the target center.
[10] W. Reisdorf, Z. Phys. A **300**, 227 (1981).
[11] M. Kicińska-Habior *et al.*, Phys. Rev. C **36**, 612 (1987).
[12] H. Nifennecker and J. A. Pinston, Annu. Rev. Nucl. Part. Sci. **40**, 113 (1990).
[13] N. Gan *et al.*, Phys. Rev. C **49**, 298 (1994).
[14] A. Lepretre *et al.*, Nucl. Phys. **A219**, 39 (1974).
[15] G. Nebbia *et al.*, Nucl. Phys. **A578**, 285 (1994).
[16] J. J. Gaardhøje *et al.*, Phys. Rev. Lett. **53**, 148 (1984).
[17] J. J. Gaardhøje *et al.*, Phys. Rev. Lett. **56**, 1783 (1986).
[18] D. R. Chakrabarty *et al.*, Phys. Rev. C **36**, 1886 (1987).
[19] K. A. Snover, in *Future Directions in Nuclear Physics with* 4Π *Gamma Detection Systems of the New Generation*, edited by J. Dudek and B. Haas, AIP Conf. Proc. No. 259 (AIP, New York, 1992), p. 299.
[20] Inelastic scattering results from E. Ramakrishnan *et al.*, Phys. Rev. Lett. **76**, 2025 (1996) have been reinterpreted in [3] and are not shown here.
[21] H. Tricoire *et al.*, Z. Phys. A **306**, 127 (1982).
[22] T. C. Awes *et al.*, Phys. Rev. C **25**, 2361 (1982); A. Gavron *et al.*, Phys. Rev. C **24**, 2048 (1981).
[23] J. Randrup and R. Vandenbosch, Nucl. Phys. **A474**, 219 (1987); R. Vandenbosch (private communication).
[24] Fig. 4 does not include the results of [5] (highest point) and [7], for which the analyses did not include bremsstrahlung, and the lowest corrected point of [5] ($\Gamma = 14.1$, $T = 2.4$ MeV), which lies anomalously high.
[25] J. J. Gaardhøje *et al.*, Phys. Rev. Lett. **59**, 1409 (1987).
[26] J. Kasagi *et al.*, Nucl. Phys. **A538**, 585c (1992).
[27] T. Suomijärvi *et al.*, Phys. Rev. C **53**, 2258 (1996).
[28] D. Kusnezov (private communication).